Journal Pre-proof

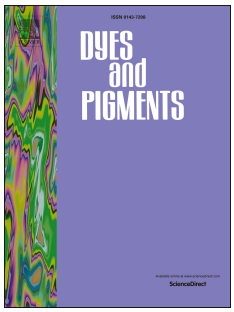

Applying styryl quinolinium fluorescent probes for imaging of ribosomal RNA in living cells

Abed Saady, Eli Varon, Avi Jacob, Yaron Shav-Tal, Bilha Fischer

PII: S0143-7208(19)32054-6

DOI: https://doi.org/10.1016/j.dyepig.2019.107986

Reference: DYPI 107986

To appear in: *Dyes and Pigments*

Received Date: 30 August 2019

Revised Date: 7 October 2019

Accepted Date: 20 October 2019

Please cite this article as: Saady A, Varon E, Jacob A, Shav-Tal Y, Fischer B, Applying styryl quinolinium fluorescent probes for imaging of ribosomal RNA in living cells, *Dyes and Pigments* (2019), doi: https://doi.org/10.1016/j.dyepig.2019.107986.

This is a PDF file of an article that has undergone enhancements after acceptance, such as the addition of a cover page and metadata, and formatting for readability, but it is not yet the definitive version of record. This version will undergo additional copyediting, typesetting and review before it is published in its final form, but we are providing this version to give early visibility of the article. Please note that, during the production process, errors may be discovered which could affect the content, and all legal disclaimers that apply to the journal pertain.

© 2019 Published by Elsevier Ltd.

Journal Pre-proof

Applying styryl quinolinium fluorescent probes for imaging of ribosomal RNA in living cells

Abed Saady[a], Eli Varon[b], Avi Jacob[b], Yaron Shav-Tal[b] and Bilha Fischer[a]*

[a] Department of Chemistry, Bar-Ilan University, Ramat-Gan 52900, Israel.

[b] Faculty of Life Sciences & Institute of Nanotechnology, Bar-Ilan University, Ramat-Gan 52900, Israel.

* Corresponding author. Fax: 972-3-6354907. Tel: 972-3-5318303.

Bar-Ilan University, Ramat-Gan 52900, Israel

E-mail: Bilha.fischer@biu.ac.il

Journal Pre-proof

Journal Pre-proof

Abstract

The detection of subcellular domains in cells can be obtained by specific fluorescent markers. Here we report the use of styryl quinolinium dyes that selectively stain ribosomal RNA (rRNA) in nucleoli and in the cytoplasm of mammalian cells. Specifically, we synthesized a series of 1-methyl-4-(substituted) styryl-quinolinium derivatives, **12a–l**. We developed highly efficient microwave-assisted synthesis which prevents the formation of side-products, leading to the products in yields greater than 90%. Compounds **12c-f** and **12i** in various solvents exhibited maximum absorbance at 500 - 660 nm, molar extinction coefficient of 25400 – 49000 $M^{-1}cm^{-1}$, and emitted at 630 - 715 nm. Dyes **12a–l** are highly photochemically stable. Dye **12e** specifically stained nucleoli and the cytoplasm and is non-toxic. Various tests showed the markedly higher affinity of the dye for rRNA. We demonstrate that **12e** is an attractive staining reagent for visualizing and assessing rRNA in both fixed and living cells.

Journal Pre-proof

Introduction

Dyes emitting at long wavelengths, green to red regions have attracted the attention of scientists for use in various applications,[1] including visualization of biomolecules in living systems, real-time tracking of cellular events, and fluorescent dye guidance during surgeries.[2-9] These applications are based on the minimal auto-fluorescence of cells at wavelengths above 600 nm, the penetration depths of NIR- dyes, as well as their sensitivity and minimal photo-damage on cells and tissues.[10-12]

Styryl quinolinium- and merocyanine- dye classes constitute scaffolds applied for the development of NIR dyes.[13] Specifically, a styryl quinolinium dye contains two non-identical aryl groups usually joined by an ethylene moiety. One of the aryl groups is electron deficient (e.g. pyridinium moiety) while the other one is electron rich, thus resulting in a push-pull system.[14] Unlike the positively charged styryl quinolinium dyes, merocyanine dyes are zwitterions and hence are essentially neutral. Merocyanine push-pull dyes contain two ethylene-bridged aryl groups, one of which is positively charged (e.g. pyridinium moiety) and the other one is negatively charged (e.g. phenolate moiety) (Fig. 1).

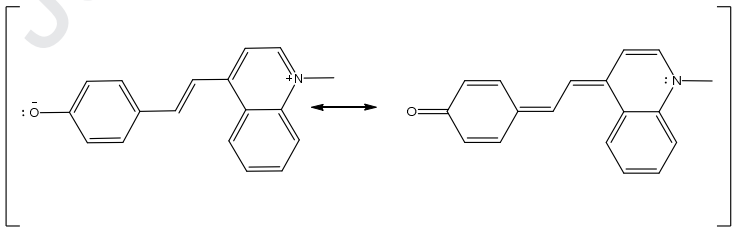

Fig. 1 Resonance structures of anion of *p*-hydroxy-styryl quinolinium dye.

Merocyanine dyes are used for detection of DNA or RNA since they often exhibit enhanced fluorescence intensity by binding to nucleic acids.[15-17]

The Knoevenagel condensation is used for production of dyes,[18] such as coumarin derivatives,[19] and styryl quinolinium derivatives, e.g. **12a** or **12b**.[20,21] The synthesis of the latter involves the reaction of 1,4-dimethyl quinolinium salts with aromatic aldehydes in ethanol or toluene under reflux for overnight, or in methanol at 50 °C for at least 3-8 h.[22] Most of these processes are time consuming and require purification of the final product, resulting in medium to good yields.

The Knoevenagel condensation is also applied for the synthesis of pharmaceuticals, such as nifedipine hypertension drugs, **1**-**3**,[23,24] 1-methyl-4-(substituted) styryl-quinolinium analogs **4**-**6** used for the treatment of tuberculosis,[25] derivatives **7**-**8**, used as choline acetyltransferase inhibitors,[26] and analog **9** which shows antitumor activity.[27] Other applications of styryl quinolinium dyes have been described.[15, 28-30]

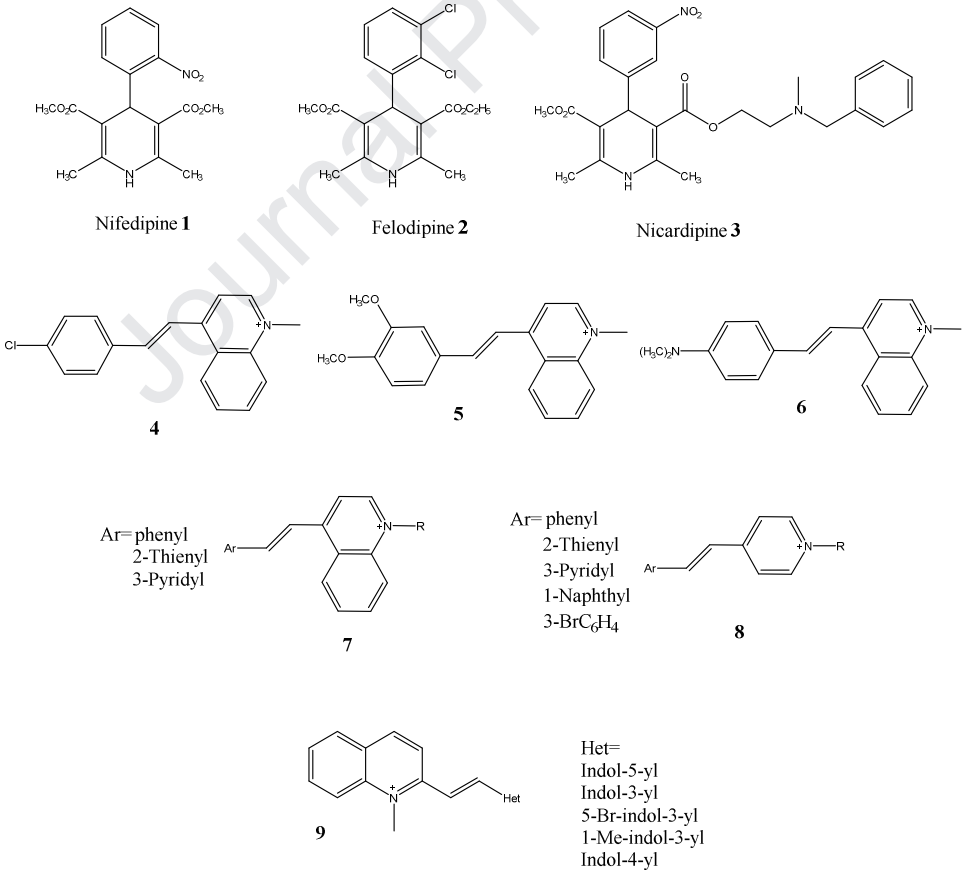

Scheme 1. Previously reported styryl-quinolinium derivatives.

The demand for new fluorescent dyes that absorb and emit above 550 nm, encouraged us to develop and characterize new dyes based on the scaffolds of merocyanine and styryl dyes. Specifically, we report here on the microwave assisted Knoevenagel condensation[31] of methyl quinolinium salt, **10**, and substituted benzaldehyde derivatives (**11a**-**11l**), to obtain (E)-2-(substituted styryl)-1,4-dimethylpyridinium iodide analogs **12a – 12l** with high efficiency.

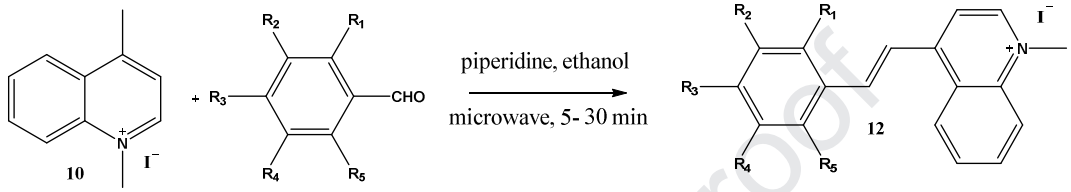

11a: R_1=H, R_2=H, R_3=OH, R_4=H, R_5=H
11b: R_1=H, R_2=H, R_3=OCH_3, R_4=H, R_5=H
11c: R_1=H, R_2=F, R_3= OH, R_4=H, R_5= H
11d: R_1=H, R_2= F, R_3=OCH_3, R_4=H, R_5=H
11e: R_1=H, R_2= F R_3= OH , R_4=F , R_5= H
11f: R_1=H, R_2=F, R_3=OCH_3, R_4=F, R_5=H
11g: R_1=F, R_2= F R_3= OH , R_4=F , R_5= F
11h: R_1=F, R_2= F R_3= OCH_3 , R_4=F , R_5= F
11i: R_1=H, R_2=H, R_3=$N(CH_3)_2$, R_4=H, R_5=H
1j: R_1=OH, R_2=H, R_3=OH, R_4=H, R_5= H
11k: R_1=OH, R_2=OCH_3, R_3=H, R_4=NO_2, R_5=H
11l: R_1=H, R_2=NO_2, R_3=OH, R_4=H, R_5= H

Scheme 2. Synthetic scheme for the preparation of **12a – 12l**.

In addition, we report on the photophysical properties and photostability of products **12a – 12l** in several solvents and pH values. The most promising dye termed **12e** was further evaluated for its photophysical properties and mode of interaction with nucleic acids in solution. Next, the safety and photostability of the compounds was studied. Finally, we describe the application of dye **12e** for rapid and selective nucleoli staining in living cells.

Results

Synthesis of dyes 12a-l

Our strategy to design new dyes was based on increasing the polarization within styryl quinolinium- and merocyanine push-pull scaffolds (Fig. 2). For instance, merocyanine analog **12a** was substituted by one or two fluorine atoms at the *ortho* positions of the phenol moiety, **12c** and **12e**, to stabilize the phenolate electron donating group. In contrast to **12c**,**e**, the phenyl moiety in **12i**, was substituted by an electron donating, dimethylamino group (Scheme 2).

For synthesizing these dyes we targeted a facile and highly efficient method. Hence, we applied microwave-assisted Knoevenagel condensation of 1,4-dimethyl quinolinium iodide, **10**,[21] and several substituted benzaldehyde derivatives, **11a-l**. Benzaldehyde derivatives **11a-d**, **11f**, and **11h-l**, are commercially available. 3,5-Difluoro-*p*-hydroxybenzaldehyde, **11e**, and 2,3,5,6-tetrafluoro-*p*-hydroxybenzaldehyde, **11g**, were synthesized from 2,6-difluorophenol,[32] and 1-(di-ethoxymethyl)-2,3,4,5,6-pentafluorobenzene,[33] respectively.

All microwave-assisted reactions in ethanol were completed in 5 - 30 min at 70-80 °C. The products were mostly obtained in a good to excellent yield (> 90%). The same reactions in ethanol under reflux were completed in 4-16 h, with lower yields (27 – 85%)[20] (Table 1).

We first explored microwave-assisted Knoevenagel condensation for the preparation of the known compounds **12a**, **12b** and **12i**.

The Knoevenagel reaction involving benzaldehyde derivatives having free hydroxyl group on the aromatic ring (**11a**, **11c**, **11e**, **11g**, **11h** and **11j**) occurs also in excellent yield and does not require any protection of the phenolic moiety.

Table 1. Comparison of the reaction time and yield of products **12a- l** obtained under microwave vs. under normal conditions.

	Microwave condition in EtOH			Normal condition in EtOH		
Product	**Yield (%)**	**Reaction time (min)**	**Temperature (°C)**	**Yield (%)**	**Reaction time (h)**	**Temperature (°C)**
12a	94	15	70	65	9	reflux
12b	96	25	80	53	6	reflux
12c	91	10	75	27	12	reflux
12d	95	15	75	55	12	reflux
12e	99	5	75	85	9	reflux
12f	90	10	75	73	14	reflux
12g	99	5	75	45	10	reflux
12h	95	15	80	37	16	reflux
12i	98	5	80	81	8	reflux
12j	94	20	80	64	12	reflux
12k	91	30	80	60	18	reflux
12l	90	30	80	59	20	reflux

Dyes **12a**–**12l** are barely soluble in nonpolar organic solvents but are readily soluble in polar organic solvents. Dyes **12a, 12c, 12e, 12g, 12j** and **12l** that bear a hydroxyl group at the *para* position of the styryl moiety, are soluble in a wide range of solvents giving colored solutions, the color of which is solvent-dependent (Fig. 3).

Journal Pre-proof

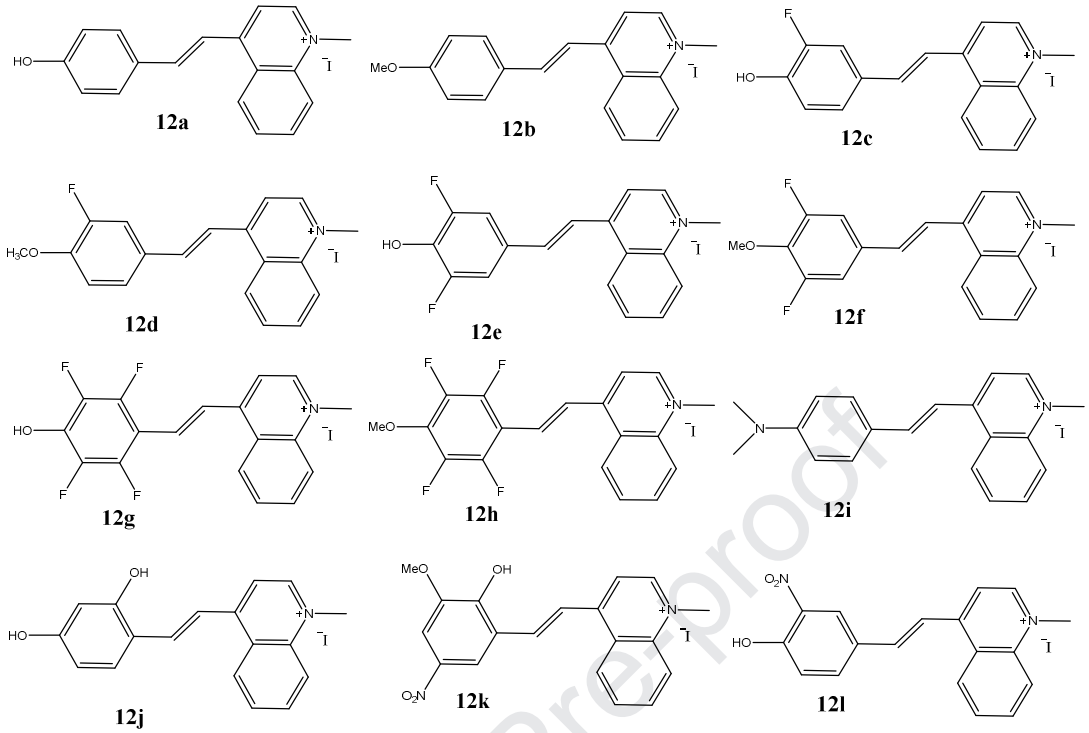

Fig 2. Styryl-quinolinium derivatives **12a-l** synthesized and evaluated in this study.

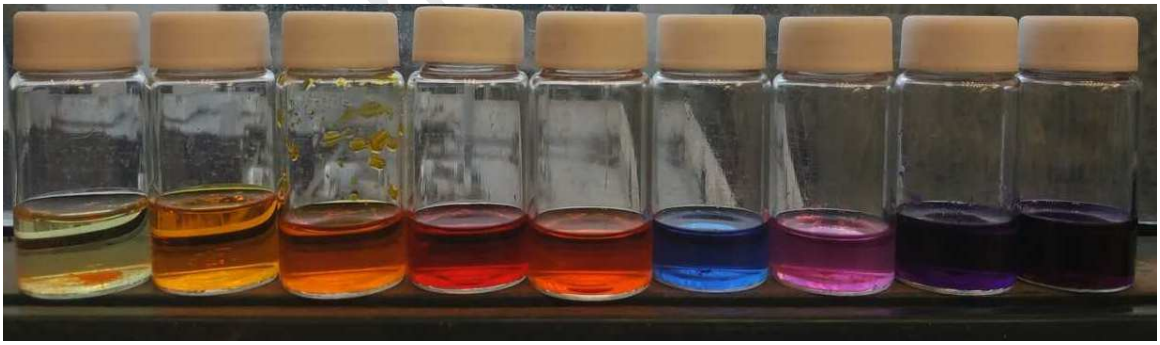

Fig. 3. Compound **12e** in various solvents, from left to right: acetic acid, water, methanol, ethanol, isopropanol, DMSO, DMF, acetone and dichloromethane.

In polar solvent such as water, the zwitterion form is dominates, while in nonpolar solvents such as chloroform, the neutral form prevails.[15]

Photophysical properties of dyes 12a-l

The photophysical properties of compounds **12a – 12l** were evaluated in various solvents at a range of relative polarity values; between 1 [34] to 0.355 (acetone)[35] (Table 2).

Table 2. Photophysical properties of derivatives **12a- 12l**.

Dye	**λ_{Abs} (nm)**	**ϵ ($M^{-1}cm^{-1}$)**	**λ_{em} (nm)**	**Dye**	**λ_{Abs} (nm)**	**ϵ ($M^{-1}cm^{-1}$)**	**λ_{em} (nm)**
Water				**MeOH**			
12a	460	21200	515	**12a**	475	22100	525
12b	438	20700	501	**12b**	440	19900	490
12c	508	26300	560	**12c**	560	27200	610
12d	502	24900	555	**12d**	508	24900	600
12e	520	45800	605	**12e**	535	46100	670
12f	515	41200	580	**12f**	520	40900	648
12g	503	23300	518	**12g**	505	23800	591
12h	478	22900	508	**12h**	490	22900	580
12i	510	29800	575	**12i**	530	30300	665
12j	470	19200	503	**12j**	478	18600	500
12k	440	16400	495	**12k**	445	17400	495
12l	475	13300	499	**12l**	480	12200	500
EtOH				**DMSO**			
12a	480	21900	525	**12a**	490	23500	528
12b	450	21300	495	**12b**	465	20600	501
12c	565	27100	640	**12c**	566	25700	660

Journal Pre-proof

12d	510	28200	605	**12d**	520	23600	610
12e	556	49000	685	**12e**	600	44700	715
12f	548	41200	665	**12f**	591	42100	675
12g	509	23900	625	**12g**	499	22950	603
12h	506	22700	608	**12h**	500	20900	595
12i	544	31000	675	**12i**	590	30100	703
12j	480	17900	495	**12j**	480	18400	500
12k	460	16900	495	**12k**	450	17900	501
12l	485	13900	506	**12l**	485	12200	509
DMF				**Acetone**			
12a	490	21500	520	**12a**	490	19900	520
12b	460	21100	500	**12b**	455	18100	505
12c	555	28100	660	**12c**	510	27600	628
12d	519	25000	610	**12d**	490	26300	605
12e	599	44900	715	**12e**	650	47100	702
12f	590	41100	675	**12f**	590	44500	685
12g	495	22100	603	**12g**	500	23200	590
12h	500	23400	595	**12h**	505	22900	590
12i	588	29800	705	**12i**	580	28300	695
12j	482	19200	503	**12j**	460	18700	495
12k	450	16400	500	**12k**	490	15800	515
12l	485	11100	505	**12l**	480	12200	508

Compound **12a** exhibits λ_{abs} at 490 nm in DMSO, while substitution of one *ortho*-hydrogen atom of the phenol with fluorine atom, **12c**, results in 76 nm red shift. Moreover, substitution of both

ortho positions of the phenol by fluorine atoms, **12e**, results in a 110 nm red shift (in DMSO). Similarly, molar extinction coefficient values (in water) are affected by fluorine atom(s) at *ortho*-position: **12a**, ϵ 21200 $M^{-1}cm^{-1}$, **12c**, ϵ 26300 $M^{-1}cm^{-1}$, **12e**, ϵ 45800 $M^{-1}cm^{-1}$. Furthermore, we explored the effect of substitution of **12a** phenol group by four fluorine atoms, **12g**, on its photophysical properties. Surprisingly, all measured parameters, $\lambda_{abs,}$ $\lambda_{em,}$ and ϵ, decreased for **12g** as compared to **12e**. For instance, while **12e** in EtOH exhibited for $\lambda_{abs,}$ $\lambda_{em,}$ and ϵ, values of 556 nm, 49000 $M^{-1}cm^{-1}$, and 685 nm, respectively; **12g** showed 509 nm, 23900 $M^{-1}cm^{-1}$, and 625 nm, respectively.

Compounds **12d** and **12f**, both contain a methoxy group in the phenol *para* position, and one fluorine atom, **12d,** or two fluorine atoms, **12f,** in the *ortho* position. We found that ϵ and λ_{abs} values of **12f** are higher than those for **12d** in all solvents. Yet, substitution of the *para* position by methoxy vs. hydroxy group, resulted in decrease of all measured parameters, $\lambda_{abs,}$ $\lambda_{em,}$ and ϵ, in all solvents, for **12f** as compared to **12e**, as well as for **12a** as compared to **12b**. These data indicate the importance of the hydroxyl group at the phenolic *para* position for improving the photophysical properties of these styryl quinolinium dyes.

We compared the effect of electron withdrawing groups at *ortho* position, e.g. nitro vs. fluoro group, on ϵ in **12l** vs. **12c**. We noticed that in most solvents ϵ values of **12l** decreased as compared to those of **12c** due to the stronger electron withdrawing effect of the nitro group.

Compound **12i** bearing a strong electron donating group at the *p*-position, $N(CH_3)_2$, shows also high $\lambda_{abs,}$ $\lambda_{em,}$ and ϵ values, about the same as for **12c**, in all solvents.

Compounds **12g, 12h, 12j** and **12k** bearing *meta* substituents – F or OH – showed poor photophysical properties.

Notably, the color of the solution of dyes containing *p*-hydroxyl group, e.g. **12a, 12c** and **12e**, (merocyanine push-pull systems) changes depending on the solvent and its polarity. In general, the more polar solvent is, the shorter is the absorption wavelength of the dye (bathochromic shift). This effect stems in part from the stabilization of the ground state of the merocyanine molecule in polar solvents, which increases the energy gap between the ground state and excited states, and corresponds to shorter wavelengths (increased energy) of the absorbed light.

Next, we evaluated the effect of pH on the absorption and emission wavelengths of **12a-l** in basic vs. acidic solutions. Dyes containing *p*-OH/NMe_2 groups exhibited red-shift of the wavelengths of absorption and emission, up to 11 nm, in basic vs. acidic medium (Table 3).

Table 3. Absorption and emission wavelengths of derivatives **12a- 12l** under acidic (pH 2) and basic conditions (pH 10).

Dye	**λ_{abs} (nm)**	**λ_{abs} (nm)**	**λ_{em} (nm)**	**λ_{em} (nm)**
	pH 2	**pH 10**	**pH 2**	**pH 10**
12a	460	467	515	522
12b	438	438	501	500
12c	508	512	560	564
12d	502	502	555	556
12e	520	531	605	608
12f	515	515	580	580
12g	503	501	518	520
12h	478	478	508	508
12i	510	508	575	578

12j	470	475	503	500
12k	440	447	495	499
12l	475	477	499	502

The quantum yields of dyes **12a-l** in all the solvents were rather low (0.0011- 0.0177). However, in glycerol ca. 3-fold increase of the quantum yield was measured. Table 4 summarizes the quantum yields of dyes **12a- 12l** in water and glycerol.

Table 4 Quantum yields of the dyes in water and glycerol.

Dye	Φ^a (%)	Φ^a (glycerol) (%)
12a	0.69	2.13
12b	0.61	1.74
12c	0.94	2.84
12d	0.87	3.47
12e	1.77	5.55
12f	1.61	4.89
12g	0.62	1.68
12h	0.48	1.09
12i	1.07	3.74
12j	0.79	2.91
12k	0.11	0.31
12l	0.28	0.92

Journal Pre-proof

[a] The fluorescence quantum yields of the dyes (2 µM) were determined in ethanol at 25 °C using rhodamine B as the standard.

The same quantum yield values were observed in MeOH, EtOH, DMF, DMSO and acetone. The high viscosity of glycerol (950 cP)[36] reduces degrees of freedom and free rotations in the dye molecules,[37] and hence allows planarity and enhanced light emission.

Photostability of dyes 12a-l

Photostability is an important requirement for the application of a fluorescent dye in biological studies. The photostability of dyes **12a-l** was tested by exposure to a light source of a Cary Eclipse Fluorescence Spectrophotometer (λ_{ex} 500–650 nm), with the exclusion of ambient light. 2µM Dye solutions in PBS were irradiated for 200 min, with an assessment of their fluorescence intensity at five-minute intervals (Fig. 5).

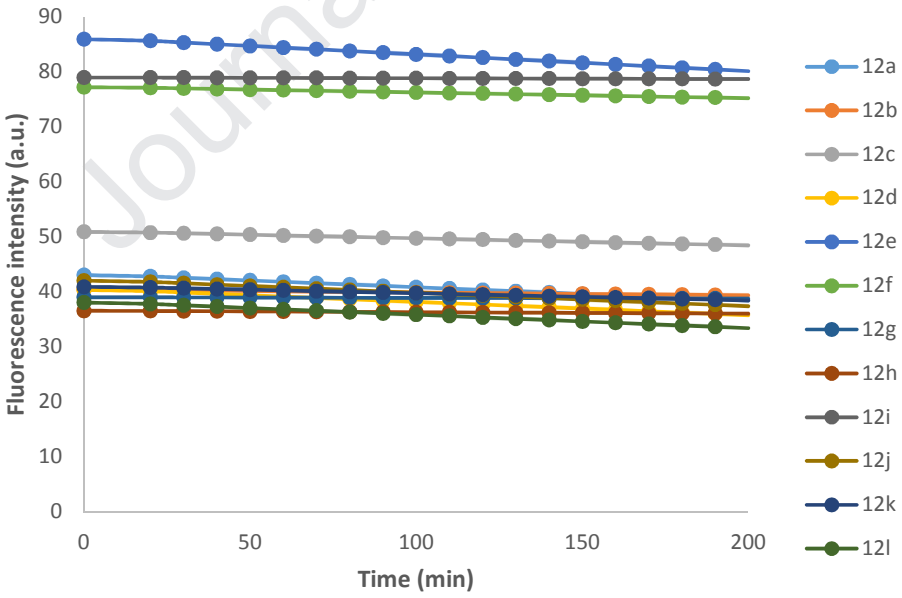

Fig. 5 Photostability of dyes **12a-l** measured by the loss of fluorescence intensity (2 µM dye, in PBS buffer).

After a 200-minute irradiation in PBS buffer, it was clearly observed that the fluorescence intensity of dyes **12a- l** was not affected by the irradiation. The remaining emission percentages of the dyes after 200 min were: **12a** (89%), **12b** (93%), **12c** (91%), **12d** (88%), **12e** (96%), **12f** (92%), **12g** (95%), **12h** (93%), **12i** (95%), **12j** (88%), **12k** (94%) and **12l** (87%). These data indicate that all the dyes have excellent photostability.

Dyes 12a-l are not toxic to cells

We evaluated the toxicity of the promising dyes on T lymphocytes by flow cytometry.[38] We measured cell death by fluorescence-activated cell sorting (FACS) which is a powerful and precise tool for measurement of a single cell within a population. We checked the cell death before adding the dyes and 3 hours after the addition of the dyes. Dyes **12c**, **12i** and **12e** were not toxic for a period of 3 hours (Fig. S1).

Dye 12e binds RNA in solution

The photostability and the most promising photophysical properties of compound **12e** encouraged us to evaluate it as a probe or staining agent for nucleic acids (RNA). This was tested by adding this dye to an RNA solution extracted from human cells and evaluating the increase in fluorescence intensity. Notably, a significant, 3.1-fold increase in fluorescence intensity was observed once compound **12e** interacted with total RNA extract (Fig. 7). Dye **12e** alone (black), RNA solution+ dye **12e** (blue), dye **12e**+ RNA solution+ RNASE, control, (green), water + RNASE, control, (red).

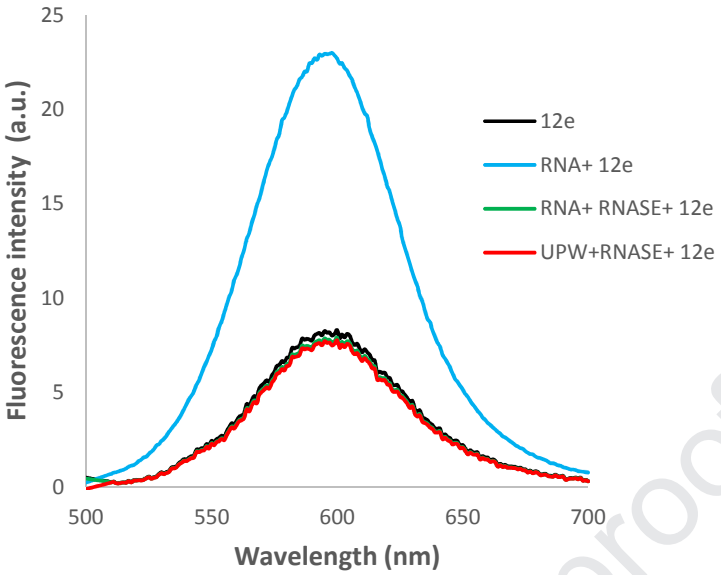

Fig. 7 Emission spectra of probe **12e** with RNA in water. Dye **12e** alone (black), RNA solution+ dye **12e** (blue), dye **12e**+ RNA solution+ RNASE, control, (green), water + RNASE, control, (red).

Dye 12e stains fixed and living cells

To analyze the fluorescent properties of compound **12e** in cells and to determine whether the dye can stably interact with RNA within the cells, we first determined the fluorescent properties of the dye in cells. We applied the dye to fixed HeLa cells and using a scanning confocal microscope equipped with a supercontinuum laser and tunable detection, we performed a lambda-lambda scan to determine the excitation-emission spectrum of the compound. We found that the peak fluorescent intensity was at the emission range of 647-667nm and optimal excitation at 570 nm, clearly showing the detection of the cells (Fig. 8A). We then measured the intensity of the signal within the images to show the spectrum as shown in Fig. 8B. Figure 8C shows a 2D heat map representing the full scan as exported from the acquisition software and

shows the peak excitation vs peak emission, as above. The signal obtained in the images at 570 nm (Fig. 8A) showed staining of several substructures in the nucleus of the cells that resembled nucleoli, while the nucleoplasm did not show signal. The cytoplasm also showed staining. This staining was observed in other cell lines as well (Fig. S2). To confirm that nucleoli were stained we performed immunofluorescent staining with a specific antibody to the nucleolar protein fibrillarin. Indeed, compound **12e** specifically stained nucleoli and the cytoplasm (Fig. 8D). Nuclei were detected with the Hoechst dye.

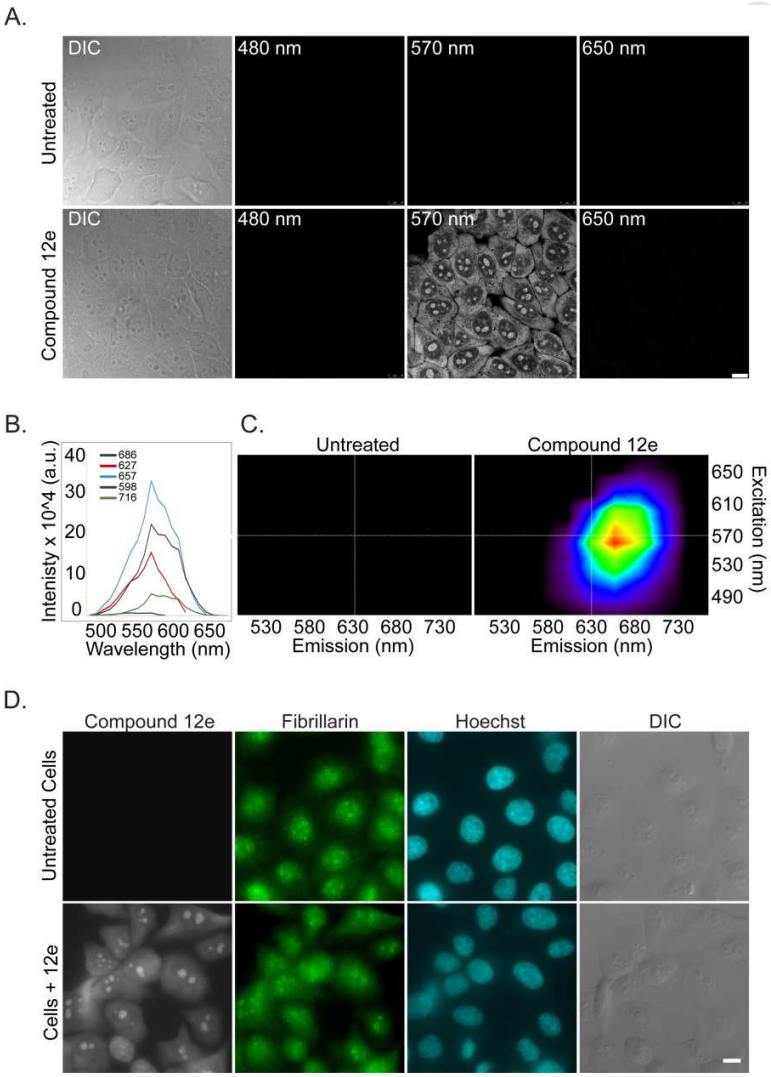

Journal Pre-proof

Fig. 8: Spectrum scan shows peak of excitation/emission. (A) Dye **12e** was added to HeLa cells and these were scanned as described in the Methods section. The strongest excitation, at the emission range of 647-667 nm was found to be 570 nm. Bar = 10 μm. (B) Images were analyzed as described in the Methods and the image emission intensities were plotted. The excitation that resulted in the strongest emission was found to be at 570 nm. (C) 2D heat map exported from acquisition software showing the excitation vs. the emission profiles. (D) Dye 12e localizes to nucleoli in treated cells. Nucleoli are identified by staining with an antibody to the nucleolar marker fibrillarin (green). Hoechst DNA stain is in cyan. No 12e signal is detected in untreated cells. Bar = 10 μm.

Since the dye stained subcellular structures in fixed cells we wanted to examine if it can be applied to living cells as well. The dye rapidly entered the cells showing that it is highly cell permeable. Within 30 seconds the compound was detected in the cytoplasm, and within 150 seconds the compound stained nucleoli (Fig. 9A). Additionally, the compound could be applied to living cells for over 24 hours without affecting viability, cell morphology, or proliferation as cell divisions continuously occurred indicating again that compound **12e** is not toxic to cells (Fig. 9B and Supplemental Movie S1). Notably, the compound remained fluorescently stable, bright and specifically bound to nucleoli (Fig. 9B), with a high signal-to-noise ratio (Fig. 9C).

Journal Pre-proof

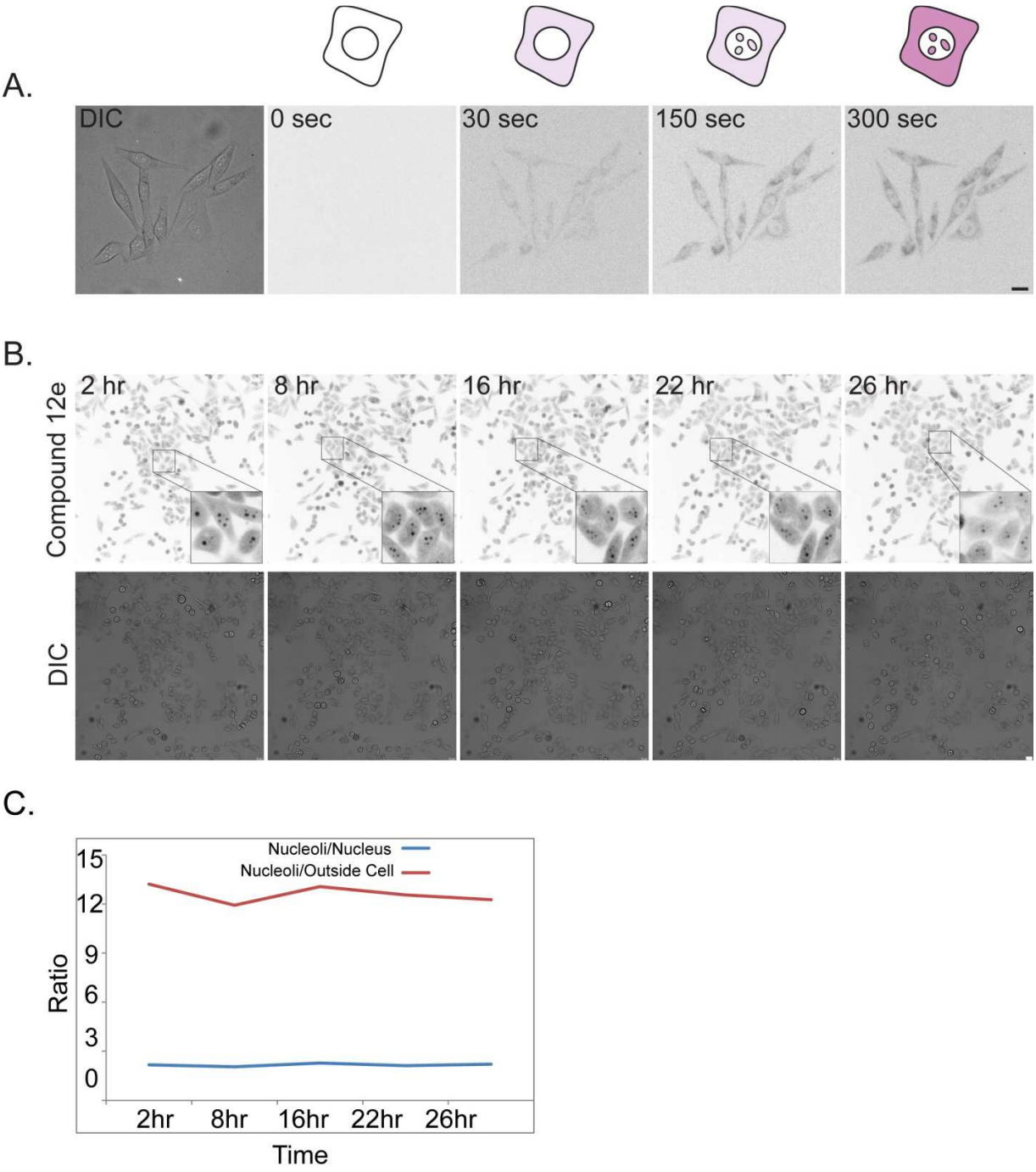

Fig. 9. Dye **12e** rapidly stains living HeLa cells and does not affect viability. (A) Cells were imaged every 5 sec for 5 min. The compound entered the cells within 30 sec and stained nucleoli within 150 sec. (B) Cells were then imaged every 15 min for 26 hrs and the compound intensity remained strong and specific to the nucleoli. The cells remained viable. Bar = 20 μm. (C) Signal-

to-noise ratio pixel intensity graph of nucleoli/nucleus and nucleoli/outside of the cell derived from ImageJ software.

Dye 12e stains fixed and living cells

The *in vitro* data suggested that compound **12e** binds to RNA. Since the nucleolus is the region in the cell where ribosomal RNA is transcribed by RNA polymerase I, we further investigated the properties of the dye to binding nucleic acids within cells. To this end, fixed and stained cells were treated with either deoxyribonuclease (DNase) or ribonuclease (RNase) to remove DNA or RNA from cells, respectively (Fig. 10). While with the treatment with DNase no considerable loss of fluorescence signal was observed (Fig. 10A), after RNase treatment, cytoplasmic and nucleolar fluorescence signal disappeared in comparison to untreated cells (Fig. 10B). These digestion experiments validated the preference of compound **12e** to attach to RNA since cells in which the RNA was removed by RNase, did not stain anymore. When the cells were treated with actinomycin D, an inhibitor of RNA polymerase II that transcribes mRNA (and not rRNA), there was not much change in the intensity of the dye in the cells, suggesting that the dye preferably binds to rRNA in the nucleolus and the cytoplasm.

Journal Pre-proof

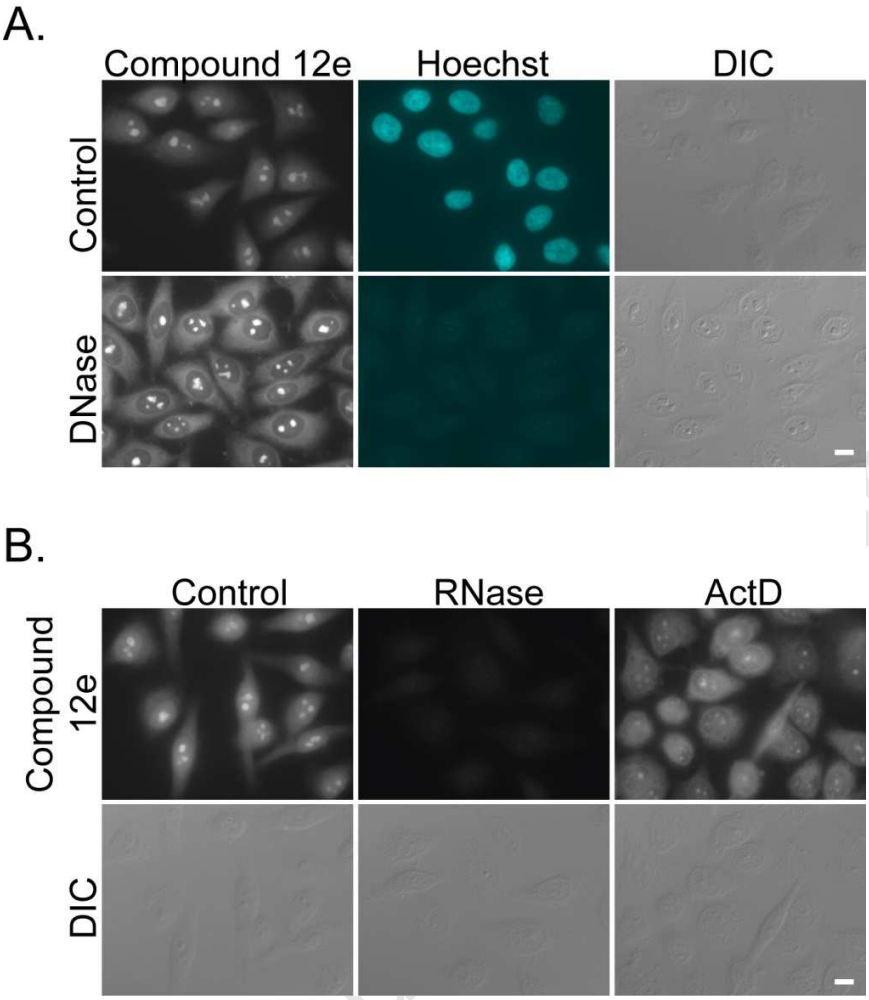

Fig. 10. Compound **12e** binds to RNA in cells. (A) Wide-field fluorescence images of untreated or DNase treated cells stained with the compound **12e**. Hoechst DNA stain is in cyan. (B) Untreated cells or cells treated with RNase or with the actinomycin D transcriptional inhibitor. DIC images are in grey. Bar = 10 μm.

To directly test the interaction of compound **12e** with rRNA, we inhibited nucleolar rRNA transcription by inhibiting RNA polymerase I activity with two specific inhibitors[33, 34, 39, 40] (Fig. 11A). Indeed, these treatments significantly reduced the fluorescent signal throughout the

nucleoli and the cytoplasm, confirming the preference of compound **12e** to rRNA. To further examine whether the compound is specific to rRNA and not mRNA, we induced the assembly of cytoplasmic stress granules that contain mRNAs but not rRNAs.[41] This way foci containing mRNAs were formed in the cytoplasm, which might be detectable by the compound if it binds mRNA. Stress granules were formed by the addition of arsenite to the cells. However, the compound did not localize with stress granules, implying that **12e** is not binding to cytoplasmic mRNA (Fig. 11B).

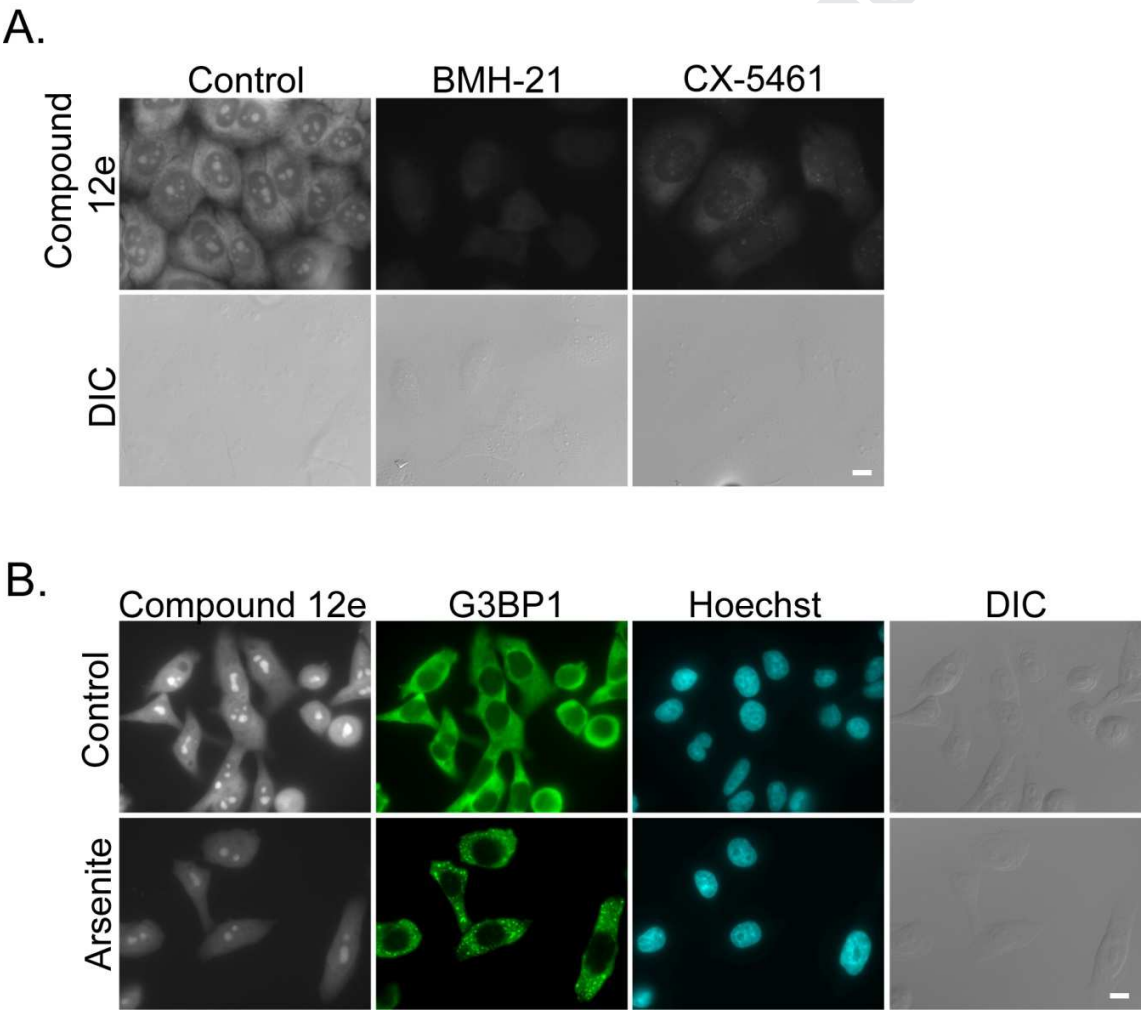

Fig. 11. Compound **12e** binds rRNA in cells. (A) Transcriptional inhibition of RNA polymerase I by CX-5461 and BMH-21 diminishes the fluorescence signal of compound **12e** in cells. (B)

Stress granules formed by arsenite treatment and labeled with anti-G3BP1 (green) do not contain compound **12e** (white). Hoechst DNA stain is in cyan. DIC is in grey. Bar = 10μm.

A main difference between rRNA and mRNA molecules is that rRNA is highly structured and contains many complex secondary structures. In order to prove that compound **12e** has preference to secondary structures in the rRNA, we purified rRNA and mRNA from total cell RNA extracts, and examined the binding of the compound to these RNAs under two conditions. At room temperature the secondary structures are preserved, and strong binding to rRNA was observed (Fig. 12). Once the secondary structures of the RNA were destroyed by heating the RNAs to 90°C, the binding to the rRNA was lost, indicating that indeed compound **12e** binds the complex secondary structures of rRNA.

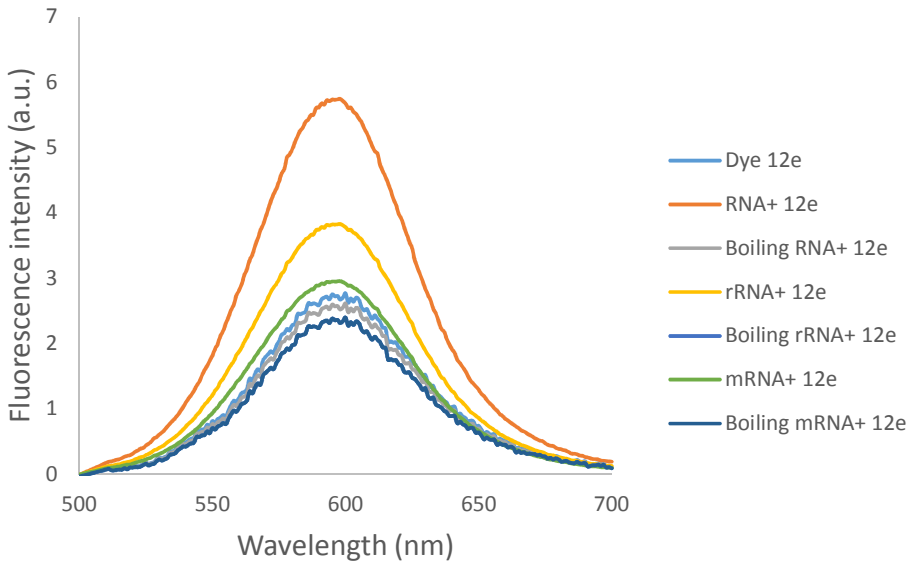

Fig. 12. Compound **12e** binds to secondary structures in rRNA. The binding of compound **12e** to rRNA and mRNA in solution at room temperature and at 90°C. In the presence of structured rRNA there is an increase in the fluorescent signal; however, when the samples were heated and

the secondary structures of the rRNA are dismantled, then no increase in fluorescence was observed.

Dye 12e binds histones-free DNA extract

Dye **12e** binds secondary structures in the rRNA that are probably double stranded (ds) however nuclear dsDNA was not stained as well. We postulated that the histones forming the nucleosomes on the DNA in cells might mask the binding of the dye. We therefore extracted DNA from cells, with or without histones, and found that dye **12e** did not bind to DNA with histones and could bind only to DNA extract in which the histones were removed (Fig. 13).

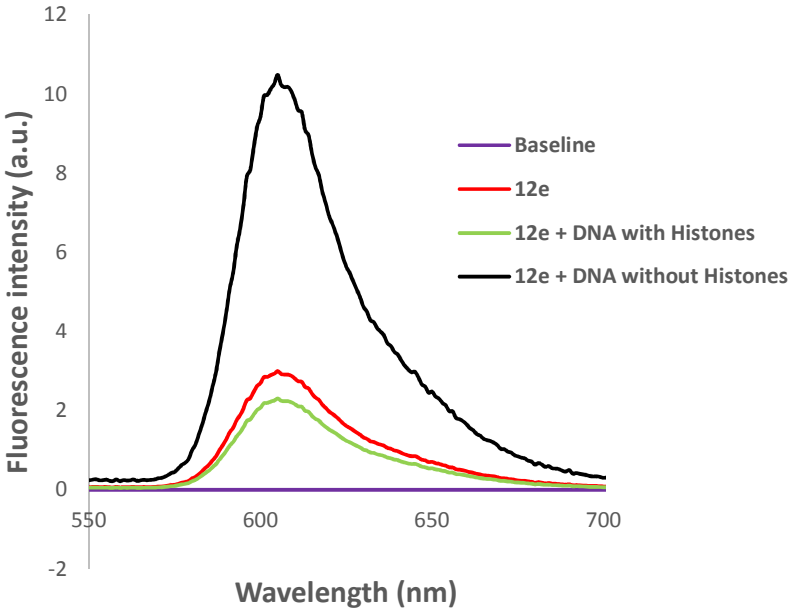

Fig. 13. Compound **12e** binds to DNA without histones

Discussion

In this study, we have synthesized and established the structure-photoactivity relationship of new and known merocyanine dyes, **12a-l** (Fig. 14).

Generally, the photophysical properties- $\lambda_{abs,}$ $\lambda_{em,}$ and ϵ- of **12a-l** were in the range of 440-658 nm; 485-715 nm; and 12,200-49,000 $M^{-1}cm^{-1}$, respectively. These values were solvent-dependent. Specifically, the more polar the solvent is, the shorter is the absorption wavelength of the dye.

The following structure-photoactivity relationships were observed: Substitution of the phenyl *para*-position with OH group enhanced photoactivity, whereas OMe group reduced it. Substitution of one or two fluorine atoms at *ortho* positions to OH/OMe groups enhanced photoactivity, due to the 1000-fold greater acidity of 2,6-difluoro-phenol than that of phenol (pK_a values of phenol and 2,6-difluoro-phenol are 9.99 and 6.88, respectively) whereas additional fluorine atoms at *meta*-position reduced overall photoactivity.

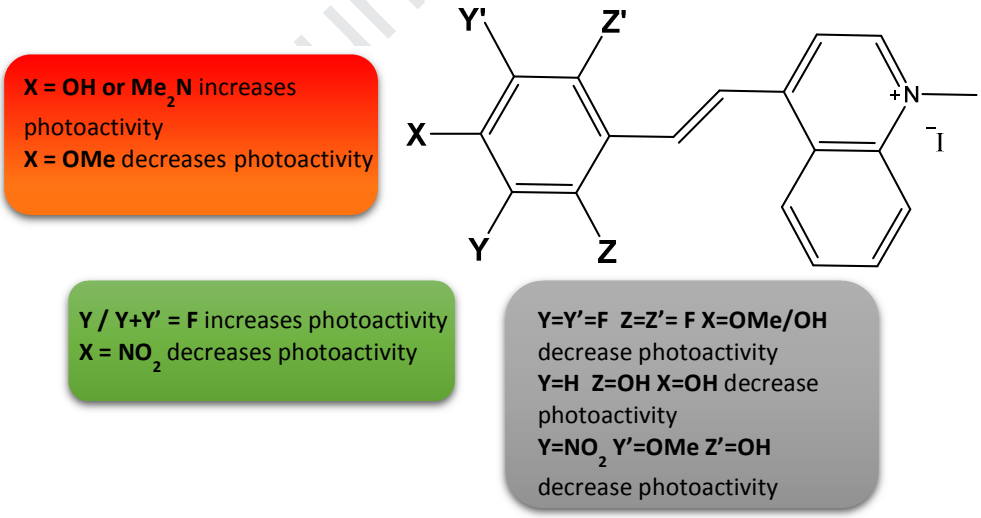

Fig. 14 Structure-photoactivity relationship in styryl-quinolinium dyes **12a-l.**

A similar observation was made for nitro or hydroxyl groups at *meta*-position. The photophysical properties of the dyes were not only polarity-dependent, but also pH-dependent (for *p*-OH substituted dyes) and viscosity-dependent. Thus, at pH 10 a bathochromic shift of maximum absorption of up to 11 nm was observed vs. that at pH 2. In glycerol the quantum yield of the compounds increased ca. 3-fold as compared to that in water. Notably, compound **12e** exhibited quantum yield of 5.5% in glycerol.

Furthermore, dyes **12a**–**l** demonstrated excellent photostability for 200 min irradiation; in particular **12e** (96% remaining).

When compound **12e**, the most promising dye, was applied to cells it showed a distinct staining pattern in the nucleoli and in the cytoplasm. Experiments within cells and *in vitro* with purified nucleic acids showed preferential binding of the dye to rRNA in the nucleolus and the cytoplasm. Moreover, we could not detect any obvious binding to mRNA *in vitro*. mRNA resides in the cytoplasm and in the nucleoplasm. Since the nucleoplasm remained unstained as were cytoplasmic stress granules that contain mRNAs, we could conclude that the dye does not bind to mRNA. The difference between rRNA and mRNA that might affect the differential binding of the dye could be the different structure of these two types of RNAs. rRNA is a highly structured molecule and indeed when its structure was disrupted at high temperature, the binding of the dye to rRNA was lost.

Dye **12e** does not stain nuclear dsDNA. We found that dye **12e** did not bind to DNA with histones and could bind only to DNA extract in which the histones were removed.

Further characterization of the dye showed its high photostability, and capability to be retained within cells for long periods with a high signal-to-noise ratio without affecting cell viability.

Various dyes have been reported for selective nucleoli staining.[42, 43] The advantages of dye **12e** over the known dyes include rapid and facile 1-step synthesis, easy purification, and rapid nucleoli staining (150 seconds).

Conclusions

In summary, we have developed here a new far-red styryl-quinolinium dye, **12e**, as a rapid and selective stain of nucleoli in both fixed and living cells. The advantages of the promising dye include: easy, rapid, efficient, and inexpensive synthetic access; water solubility; selective fluorescence enhancement in the presence of rRNA; no effect on cell viability; and high photo-stability.

Experimental

Materials and Methods

Reagents and solvents were purchased from commercial sources and were used without further purification. The quaternary salts were prepared as previously reported in the literature by reflux in 1,4-dioxane of the starting compounds with iodomethane.[44] All reactants in moisture sensitive reactions were dried overnight in a vacuum oven. Progress of reactions was monitored by TLC on precoated Merck silica gel plates (60F-254). Visualization was accomplished by UV light. Compounds were characterized by nuclear magnetic resonance using Bruker, DPX-300 and DMX-600 spectrometers. ^{1}H, ^{13}C, DEPT, ^{19}F NMR spectra were measured. Compounds were analyzed under ESI (electron spray ionization) conditions on a Q-TOF micro-instrument (Waters, UK). Absorption spectra were measured on a UV-2401PC UV-VIS recording spectrophotometer (Shimadzu, Kyoto, Japan). Emission spectra were measured using Cary

Eclipse Fluorescence Spectrophotometer. The fluorescence quantum yields of the dyes were determined relative to rhodamine B in ethanol at 25 °C. The quantum yield was calculated according to the following equation:

$$\Phi_F = \Phi_R \, I / I_R * OD_R / OD * \eta^2 / \eta_R$$

Here, Φ and Φ_R are the fluorescence quantum yield of the sample and the reference, respectively, I and I_R are areas under the fluorescence spectra of the sample and of the reference, respectively, OD and OD_R are the absorption values of the sample and the reference at the excitation wavelength, and η and η_R are the refractive index for the respective solvents used for the sample and the reference. The photostability of all the dyes was tested by exposure to a light source of a Cary Eclipse Fluorescence Spectrophotometer, with the exclusion of ambient light. 2μM Dye solutions in PBS were irradiated for 200 min, with an assessment of their fluorescence intensity at five-minute intervals

General synthetic procedure

To a 10 mL microwave reaction vessel equipped with a magnetic stirring bar were added 1,4-dimethyl quinolinium iodide (0.5 mmol), absolute ethanol (5 mL), piperidine (cat. amount), and substituted benzaldehyde (0.5 mmol). The vessel was sealed, and the mixture was irradiated in a microwave oven (CEM Focused Microwave type Discover) for 5 to 30 min at 70–80 °C (as indicated in Table 1). Then the reaction mixture was cooled to RT, and diethyl ether (10 mL) was added to precipitate the products as black crystals. The latter were vacuum-filtered and washed 3x3 mL with diethyl ether to yield pure products. Products **12a-l** were >95% pure as determined by ^{1}H NMR, ^{13}C NMR, ^{19}F NMR, DEPT, UV and HRMS.

Selected Data

3,5-Difluoro-4-hydroxybenzaldehyde. ^{1}H-NMR (400 MHz, $CDCl_3$): 9.82 (t, J = 1.8 Hz, 1H), 7.49 (d, J = 6.4 Hz, 2H). ^{13}C NMR (ppm): 190.93, 152.32, 137.15, 132.74, 111.53. ^{19}F NMR (376 MHz, $CDCl_3$) δ -135.14 ppm. HRMS Calcd for $C_7H_4F_2O_2$ m/z 158.03035, Found 158.03024.

2,3,5,6-Tetrafluoro-4-hydroxybenzaldehyde. ^{1}H NMR (DMSO, 400 MHz): δ 10.22 (s, 1 H), 3.36 (bs, 1H). ^{13}C NMR (DMSO 75.45 MHz): δ 91.5, 98.7, 136.1, 139.5, 143.2, 146.5, 182.3. Calcd for $C_7H_2F_4O_2$ m/z 194.09183, Found 193.09189.

(E)-2-(4-hydroxystyryl)-1,4-dimethylpyridinium iodide (12a). ^{1}H-NMR (400 MHz, DMSO (d6)): 8.97 (d, 5.89 Hz, 1H, Ar), 8.68 (d, 8.5 Hz, 1H, Ar), 7.93 (d, 16.1 Hz, 1H, CH=CH), 7.91 (d, 16.1 Hz, 1H, CH=CH), 7.8 (d, 7.8 Hz, 1H, Ar), 7.66 (dd, 8.5, 7.8 Hz, 1H, Ar), 7.57 (d, 5.8 Hz, 1H, Ar), 7.31 (d, 8.72 Hz, 2H, Ar), 7.16 (dd, 8.5, 7.8 Hz, 1H, Ar), 6.95 (d, 8.72 Hz, 2H, Ar), 4.31 (s, 3H, $^{+}NCH_3$). ^{13}C NMR (ppm): 157.71, 157.32, 142.85, 132.54, 130.83, 130.52, 129.98, 129.54, 128.14, 126.91, 126.71, 125.02, 123.82, 119.87, 116.16, 115.95, 46.92. HRMS Calcd for $C_{18}H_{16}NOI$ *m/z* 389.23025, Found 389.23024.

(E)-2-(4-Methoxystyryl)-1,4-dimethylpyridinium iodide (12b). ^{1}H-NMR (400 MHz, DMSO (d6)): 8.96 (d, 5.89 Hz, 1H, Ar), 8.68 (d, 8.5 Hz, 1H, Ar), 7.93 (d, 16.1 Hz, 1H, CH=CH), 7.91 (d, 16.1 Hz, 1H, CH=CH), 7.8 (d, 7.8 Hz, 1H, Ar), 7.66 (dd, 8.5, 7.8 Hz, 1H, Ar), 7.57 (d, 5.8 Hz, 1H, Ar), 7.31 (d, 8.72 Hz, 2H, Ar), 7.16 (dd, 8.5, 7.8 Hz, 1H, Ar), 6.95 (d, 8.72 Hz, 2H, Ar), 4.31 (s, 3H, $^{+}NCH_3$), 3.92 (s, 3H, OCH_3). ^{13}C NMR (ppm): 157.71, 157.32, 142.85, 132.54,

130.83, 130.52, 129.98, 129.54, 128.14, 126.91, 126.71, 125.02, 123.82, 119.87, 116.16, 115.95, 55.52, 46.92. HRMS Calcd for $C_{19}H_{18}NOI$ *m/z* 403.48018, Found 403.48026.

(E)-2-(3-Flouro-4-hydroxystyryl)-1,4-dimethylpyridinium iodide (12c). ^{1}H-NMR (400 MHz, DMSO (d6)): 9.06 (d, 5.89 Hz, 1H, Ar), 8.68 (d, 8.5 Hz, 1H, Ar), 8.43 (d, 16.1 Hz, 1H, CH=CH), 7.91 (d, 16.1 Hz, 1H, CH=CH), 7.8 (d, 7.8 Hz, 1H, Ar), 7.66 (dd, 8.5, 7.8 Hz, 1H, Ar), 7.57 (d, 5.8 Hz, 1H, Ar), 7.31 (d, 8.72 Hz, 2H, Ar), 7.16 (dd, 8.5, 7.8 Hz, 1H, Ar), 6.95 (d, 8.72 Hz, 1H, Ar), 4.31 (s, 3H, $^{+}NCH_3$).^{13}C NMR (ppm): 157.81, 153.33, 147.45, 146.94, 139.83, 136.62, 133.44, 129.98, 126.14, 125.14, 124.91, 123.76, 123.09, 122.12, 118.67, 117.46, 112.65, 45.32. ^{19}F NMR -130.94 ppm. HRMS Calcd for $C_{18}H_{15}FNOI$ *m/z* 407.22431, Found 407.21909.

(E)-2-(3-Flouro-4-methoxystyryl)-1,4-dimethylpyridinium iodide (12d). ^{1}H-NMR (400 MHz, DMSO (d6)): 9.06 (d, 5.89 Hz, 1H, Ar), 8.68 (d, 8.5 Hz, 1H, Ar), 8.43 (d, 16.1 Hz, 1H, CH=CH), 7.91 (d, 16.1 Hz, 1H, CH=CH), 7.8 (d, 7.8 Hz, 1H, Ar), 7.66 (dd, 8.5, 7.8 Hz, 1H, Ar), 7.57 (d, 5.8 Hz, 1H, Ar), 7.31 (d, 8.72 Hz, 2H, Ar), 7.16 (dd, 8.5, 7.8 Hz, 1H, Ar), 6.95 (d, 8.72 Hz, 1H, Ar), 4.31 (s, 3H, $^{+}NCH_3$), 3.82 (s, 3H, OCH_3).^{13}C NMR (ppm): 157.81, 153.33, 147.45, 146.94, 139.83, 136.62, 133.44, 129.98, 126.14, 125.14, 124.91, 123.76, 123.09, 122.12, 118.67, 117.46, 112.65, 55.23, 45.32. ^{19}F NMR -129.83 ppm. HRMS Calcd for $C_{19}H_{17}FNOI$ *m/z* 421.49363, Found 421.51019.

(E)-2-(3, 5-Difluoro-4-hydroxystyryl)-1,4-dimethylpyridinium iodide (12e). ^{1}H-NMR (400 MHz, DMSO (d6)): 9.02 (d, 5.8 Hz, 1H, Ar), 8.68 (d, 8.5 Hz, 1H, Ar), 7.93 (d, 16.1 Hz, 1H, CH=CH), 7.91 (d, 16.1 Hz, 1H, CH=CH), 7.8 (d, 7.8 Hz, 1H, Ar), 7.66 (dd, 8.5, 7.8 Hz, 1H, Ar),

7.57 (d, 5.8 Hz, 1H, Ar), 7.31 (d, 8.72 Hz, 2H, Ar), 7.16 (dd, 8.5, 7.8 Hz, 1H, Ar), 4.31 (s, 3H, $^{+}NCH_3$). ^{13}C NMR (ppm): 157.81, 153.33, 147.45, 146.94, 139.83, 136.62, 133.44, 129.98, 126.14, 125.14, 124.91, 123.76, 123.09, 122.12, 118.67, 117.46, 112.65, 45.32. ^{19}F NMR -133.13 ppm. HRMS Calcd for $C_{18}H_{14}F_2NOI$ *m/z* 425.22031, Found 425.21901.

(E)-2-(3, 5-Difluoro-4-methoxystyryl)-1,4-dimethylpyridinium iodide (12f). ^{1}H-NMR (400 MHz, DMSO (d6)): 9.02 (d, 5.8 Hz, 1H, Ar), 8.68 (d, 8.5 Hz, 1H, Ar), 7.93 (d, 16.1 Hz, 1H, CH=CH), 7.91 (d, 16.1 Hz, 1H, CH=CH), 7.8 (d, 7.8 Hz, 1H, Ar), 7.66 (dd, 8.5, 7.8 Hz, 1H, Ar), 7.57 (d, 5.8 Hz, 1H, Ar), 7.31 (d, 8.72 Hz, 2H, Ar), 7.16 (dd, 8.5, 7.8 Hz, 1H, Ar), 4.31 (s, 3H, $^{+}NCH_3$), 3.83 (s, 3H, OCH_3). ^{13}C NMR (ppm): 157.81, 153.33, 147.45, 146.94, 139.83, 136.62, 133.44, 129.98, 126.14, 125.14, 124.91, 123.76, 123.09, 122.12, 118.67, 117.46, 112.65, 62.35, 45.32. ^{19}F NMR -133.13 ppm. HRMS Calcd for $C_{19}H_{16}F_2NOI$ *m/z* 439.14021, Found 439.15001.

(E)-2-(2,3,5,6-Tetrafluoro-4-hydroxystyryl)-1,4-dimethylpyridinium iodide (12g). ^{1}H-NMR (400 MHz, DMSO (d6)): 9.02 (d, 5.8 Hz, 1H, Ar), 8.63 (d, 7.8 Hz, 1H, Ar), 8.41 (d, 5.4 Hz, 1H, Ar), 8.23 (dd, 7.8, 5.4 Hz, 1H, Ar), 8.11 (dd, 8.5, 7.8 Hz, 1H, Ar), 7.84 (d, 5.8 Hz, 1H, Ar), 7.22 (d, 16.1 Hz, 1H, CH=CH), 6.78 (d, 16.1 Hz, 1H, CH=CH), 4.31 (s, 3H, $^{+}NCH_3$). ^{13}C NMR (ppm): 157.81, 153.33, 147.45, 146.94, 139.83, 136.62, 133.44, 129.98, 126.14, 125.14, 124.91, 123.76, 123.09, 122.12, 118.67, 117.46, 112.65, 45.32. ^{19}F NMR -156.27, -133.13 ppm. HRMS Calcd for $C_{18}H_{12}F_4NOI$ *m/z* 461.77062, Found 461.77059.

(E)-2-(2,3,5,6-Tetrafluoro-4-methoxystyryl)-1,4-dimethylpyridinium iodide (12h). The dye was not sufficiently soluble in any solvent in order to perform NMR tests. HRMS Calcd for $C_{19}H_{14}F_4NOI$ *m/z* 475.26041, Found 475.26039.

(E)-2-(4-Dimethylaminostyryl)-1,4-dimethylpyridinium iodide (12i). ^{1}H-NMR (400 MHz, DMSO (d6)): 9.11 (d, 5.89 Hz, 1H, Ar), 8.68 (d, 8.5 Hz, 1H, Ar), 7.93 (d, 16.1 Hz, 1H, CH=CH), 7.91 (d, 16.1 Hz, 1H, CH=CH), 7.8 (d, 7.8 Hz, 1H, Ar), 7.66 (dd, 8.5, 7.8 Hz, 1H, Ar), 7.57 (d, 5.8 Hz, 1H, Ar), 7.31 (d, 8.72 Hz, 2H, Ar), 7.16 (dd, 8.5, 7.8 Hz, 1H, Ar), 6.95 (d, 8.72 Hz, 2H, Ar), 4.42 (s, 3H, $^+NCH_3$), 3.01 (s, 6H, $N(CH_3)_2$). 157.71, 157.32, 142.85, 132.54, 130.83, 130.52, 129.98, 129.54, 128.14, 126.91, 126.71, 125.02, 123.82, 119.87, 116.16, 115.95, 46.92, 41.39. HRMS Calcd for $C_{20}H_{21}N_2I$ *m/z* 416.71421, Found 416.71409.

(E)-2-(3,4-Dihydroxystyryl)-1,4-dimethylpyridinium iodide (12j). ^{1}H-NMR (400 MHz, DMSO (d6)): 9.02 (d, 5.89 Hz, 1H, Ar), 8.68 (d, 8.5 Hz, 1H, Ar), 7.93 (d, 16.1 Hz, 1H, CH=CH), 7.91 (d, 16.1 Hz, 1H, CH=CH), 7.8 (d, 7.8 Hz, 1H, Ar), 7.57 (d, 5.8 Hz, 1H, Ar), 7.29 (s, 1H, Ar), 7.17 (s, 1H, Ar), 7.16 (dd, 8.5, 7.8 Hz, 1H, Ar), 6.95 (d, 8.72 Hz, 2H, Ar), 6.64 (s, 1H, Ar), 4.31 (s, 3H, $^+NCH_3$).^{13}C NMR (ppm): 160.6, 157.42, 146.32, 140.05, 139.51, 136.83, 133.44, 126.08, 125.84, 125.61, 124.91, 124.03, 123.99, 123.82, 122.87, 119.35, 118.95, 111.77, 46.02. HRMS Calcd for $C_{18}H_{15}BrNOI$ *m/z* 405.13662, Found 405.13648.

(E)-2-(2-Hydroxy-3-methoxy-5-nitrostyryl)-1,4-dimethylpyridinium iodide (12k). The dye was not sufficiently soluble in any solvent in order to perform NMR tests. HRMS Calcd for $C_{19}H_{17}N_2O_4I$ *m/z* 464.26553, Found 464.25919.

(E)-2-(4-Hydroxy-3-nitrostyryl)-1,4-dimethylpyridinium iodide (12l). ^{1}H-NMR (400 MHz, DMSO (d6)): 9.06 (d, 5.89 Hz, 1H, Ar), 8.68 (d, 8.5 Hz, 1H, Ar), 8.43 (d, 16.1 Hz, 1H, CH=CH), 7.91 (d, 16.1 Hz, 1H, CH=CH), 7.8 (d, 7.8 Hz, 1H, Ar), 7.66 (dd, 8.5, 7.8 Hz, 1H, Ar), 7.57 (d, 5.8 Hz, 1H, Ar), 7.31 (d, 8.72 Hz, 2H, Ar), 7.16 (dd, 8.5, 7.8 Hz, 1H, Ar), 6.95 (d, 8.72 Hz, 1H, Ar), 4.31 (s, 3H, $^{+}NCH_3$).^{13}C NMR (ppm): 157.81, 153.33, 147.45, 146.94, 139.83, 136.62, 133.44, 129.98, 126.14, 125.14, 124.91, 123.76, 123.09, 122.12, 118.67, 117.46, 112.65, 45.32. HRMS Calcd for $C_{18}H_{15}N_2O_3I$ *m/z* 434.02911, Found 434.028922.

Cell Culture

Human U2OS cells were cultured under standard conditions at 37 °C, 5% CO2, in low glucose Dulbecco's modified Eagle's medium (DMEM, Biological Industries, Israel) containing 10% fetal bovine serum (FBS, HyClone), and 4 mM Glutamine, 100 IU/mL Penicillin, and 100µg/mL Streptomycin (Biological Industries). HeLa, HEK293, and mouse embryonic fibroblasts (MEF) were maintained in high glucose DMEM containing 10% FBS, and 100 IU/mL Penicillin, and 100µg/mL Streptomycin. For RNase digestion, cells were treated with 5 µg/ml actinomycin D (Sigma) for 3 hrs, then fixed in ice cold methanol for 2min, and digested with RNase (100 mg/ml in PBS with 3 mM $MgCl_2$, Sigma) for 45min at room temperature. For DNase treatment, cells were first fixed in ice cold methanol for 2 min, and then incubated (100 mg/ml, 5 mM $MgCl_2$) for 2 hrs at room temperature. Nuclei were counterstained with 1µM Hoechst 33342 (Sigma) and coverslips were mounted in mounting medium.

Compound 12e (10 µg/mL) was added to cells after fixation for 10 min with 4% PFA for 20 min and then washed briefly with PBS. The cells were then mounted in mounting medium and

imaged. Stress granules were formed by adding arsenite (1 Mm, Sigma) to the medium for up to 45 min. For RNA polymerase I inhibition 1μM CX-5461 (AdooQ BioScience) and 1μM BMH-21 (Sigma) were incubated with cells for 48 hours.

Immunofluorescence

Cells were grown on coverslips, washed with PBS and fixed for 20 min in 4% PFA. Cells were then permeabilized in 0.5% Triton X-100 for 2.5 min. Cells were washed twice with PBS and blocked with 5% BSA for 20 min, and immunostained for 1 hr with a primary antibody. After three washes with PBS, the cells were incubated for 1 hr with secondary fluorescent antibodies. Primary antibodies: mouse anti-G3BP1 (Abcam) and rabbit anti-fibrillarin (Abcam). Secondary antibodies: Alexa Fluor 488 goat anti-mouse (Abcam) Alexa Flour 488 goat anti-rabbit (Abcam). Cells were then stained with compound 12e (10 μg/mL). Nuclei were counterstained with 1μM Hoechst 33342 (Sigma) and coverslips were mounted in mounting medium.

Fluorescence microscopy

For spectral scanning, we used an inverted Leica SP8 scanning confocal microscope, driven by the LASX software (Leica Microsystems, Mannheim, Germany) and equipped with a super-continuum white light laser. A lambda-lambda scan was performed with the software, with a PL APO 63x/1.40 OIL objective. After export, images were analysed with Cell Profiler[45] to measure the intensity of the images, and data was exported to Excel and plotted. For live cell imaging, a Leica DMI8 wide-field inverted microscope was used, equipped with a Leica sCMOS camera and CO2/incubation system. Cells were imaged every 5 seconds for the short time course, and every 15 min for the longer time course. Wide-field fluorescence images of fixed cells were

obtained using the Cell^R system based on an Olympus IX81 fully motorized inverted microscope (60X PlanApo objective, 1.42 NA) fitted with an Orca-AG CCD camera (Hamamatsu) driven by the Cell^R software. ImageJ software was used when measuring the signal-to-noise ratio graph by acquiring the intensity of several pixels from each time point**.**

RNA extraction

Total RNA was produced by using Tri-Reagent (Sigma), and DNA was removed using Turbo-DNase free kit (Invitrogen). 2 μg of total RNA extracts from HeLa cells were separated by electrophoresis in a 1% agarose gel. The rRNA 28S and 18S bands were extracted separately from the smeared mRNA in the gel. RNAs were cleaned with a Nucleospin gel and PCR clean up kit (Macherey-Nagel).

DNA and chromatin protein extraction

Genomic DNA lacking nucleosomes was purified from HEK293 cells using the TIANamp Genomic kit (TIANGEN, China). Genomic DNA including nucleosomes was purified from HEK293T cells as follows. Cells were washed with PBS and collected at 500 × g for 5 min and then lysed in Nonidet P-40 lysis buffer (25 mM Tris-HCl, pH 7.4, 150 mM NaCl, 10% glycerol and 1% Nonidet P-40) with a protease inhibitor cocktail (1:100 dilution) at 4 °C for 5 min. After centrifugation at 15,000 × g for 5 min, the pellets were collected and washed with Nonidet P-40 lysis buffer. Then Nonidet P-40 lysis buffer with micrococal nuclease (1:100 BioLabs), 5mM $CaCl_2$ and a protease inhibitor cocktail (1:100 dilution) were added to the pellets and incubated

at 25 °C for 10 min. 10 mM EGTA was added to stop the reaction. After centrifugation at 15,000 × g for 15 min, the supernatant containing the chromatin were collected.

Acknowledgments

Research supported by the Ministry of Science Technology & Space, Israel. We thank Matan Avivi and Haim Cohen (Bar Ilan University) for the nucleosome extraction from HEK 293 cells. We thank Ronit Sarid (Bar Ilan University) for providing us with reagents.

Conflict of interest

The authors declare no conflicts of interest.

Journal Pre-proof

References

1. D Nolting, D.; C Gore, J.; Pham, W., Near-infrared dyes: probe development and applications in optical mole-cular imaging. *Curr. Org. Chem* **2011,** *8* (4), 521-534.
2. Spa, S.; Hensbergen, A.; van der Wal, S.; Kuil, J.; van Leeuwen, F., The influence of systematic structure alterations on the photophysical properties and conjugation characteristics of asymmetric cyanine 5 dyes. *Dyes Pigm.* **2018,** *152*, 19-28.
3. Ferrari, E.; Gu, C.; Niranjan, D.; Restani, L.; Rasetti-Escargueil, C.; Obara, I.; Geranton, S. M.; Arsenault, J.; Goetze, T. A.; Harper, C. B., Synthetic self-assembling clostridial chimera for modulation of sensory functions. *Bioconjug Chem* **2013,** *24* (10), 1750-1759.
4. van Leeuwen, F. W.; Hardwick, J. C.; van Erkel, A. R., Luminescence-based imaging approaches in the field of interventional molecular imaging. *Radiology* **2015,** *276* (1), 12-29.
5. Byrne, W. L.; DeLille, A.; Kuo, C.; de Jong, J. S.; van Dam, G. M.; Francis, K. P.; Tangney, M., Use of optical imaging to progress novel therapeutics to the clinic. *J. Control. Release* **2013,** *172* (2), 523-534.
6. Niu, G.; Liu, W.; Xiao, H.; Zhang, H.; Chen, J.; Dai, Q.; Ge, J.; Wu, J.; Wang, P., Keto-benzo [h]-Coumarin-Based Near-Infrared Dyes with Large Stokes Shifts for Bioimaging Applications. *Chem Asian J* **2016,** *11* (4), 498-504.
7. Massoud, T. F.; Gambhir, S. S., Molecular imaging in living subjects: seeing fundamental biological processes in a new light. *Genes Dev.* **2003,** *17* (5), 545-580.
8. Weissleder, R., Molecular imaging in cancer. *Science* **2006,** *312* (5777), 1168-1171.
9. Kircher, M. F.; Gambhir, S. S.; Grimm, J., Noninvasive cell-tracking methods. *Nat. Rev. Clin. Oncol* **2011,** *8* (11), 677.
10. Weissleder, R.; Mahmood, U., Molecular imaging. *Radiology* **2001,** *219* (2), 316-333.
11. Hilderbrand, S. A.; Weissleder, R., Near-infrared fluorescence: application to in vivo molecular imaging. *Curr Opin Chem Biol* **2010,** *14* (1), 71-79.
12. Yuan, L.; Lin, W.; Zheng, K.; He, L.; Huang, W., Far-red to near infrared analyte-responsive fluorescent probes based on organic fluorophore platforms for fluorescence imaging. *Chem. Soc. Rev.* **2013,** *42* (2), 622-661.
13. Yang, E.; Zhang, N.; Krayer, M.; Taniguchi, M.; Diers, J. R.; Kirmaier, C.; Lindsey, J. S.; Bocian, D. F.; Holten, D., Integration of Cyanine, Merocyanine and Styryl Dye Motifs with Synthetic Bacteriochlorins. *Photochem. Photobiol.* **2016,** *92* (1), 111-125.
14. Nano, A.; Ziessel, R.; Stachelek, P.; Harriman, A., Charge-Recombination Fluorescence from Push–Pull Electronic Systems Constructed around Amino-Substituted Styryl–BODIPY Dyes. *Chem.: Eur. J.* **2013,** *19* (40), 13528-13537.
15. Mishra, A.; Behera, R. K.; Behera, P. K.; Mishra, B. K.; Behera, G. B., Cyanines during the 1990s: a review. *Chem. Rev.* **2000,** *100* (6), 1973-2012.
16. Dash, S.; Panigrahi, M.; Baliyarsingh, S.; K Behera, P.; Patel, S.; K Mishra, B., Cyanine dyes-nucleic acids interactions. *Curr. Org. Chem.* **2011,** *15* (15), 2673-2689.
17. Levitus, M.; Ranjit, S., Cyanine dyes in biophysical research: the photophysics of polymethine fluorescent dyes in biomolecular environments. *Q. Rev. Biophys.* **2011,** *44* (1), 123-151.
18. Seiad, L. L.; Villemin, D.; Bar, N.; Hachemi, M., Solvent-Free condensation of methyl pyridinium and quinolinium salts with aldehydes catalyzed by DBU. *Synth. Commun.* **2012,** *42* (5), 650-657.
19. Ramani, A.; Chanda, B.; Velu, S.; Sivasanker, S., One-pot synthesis of coumarins. Catalysis by the solid base, calcined Mg-Al hydrotalcite. *Green Chem* **1999,** *1* (3), 163-165.
20. Li, Y.; Xu, D.; Ho, S.-L.; Li, H.-W.; Yang, R.; Wong, M. S., A theranostic agent for in vivo near-infrared imaging of β-amyloid species and inhibition of β-amyloid aggregation. *Biomaterials* **2016,** *94*, 84-92.
21. Teshome, A.; Bhuiyan, M. D. H.; Gainsford, G. J.; Ashraf, M.; Asselberghs, I.; Williams, G. V.; Kay, A. J.; Clays, K., Synthesis, linear and quadratic nonlinear optical properties of ionic indoline and N, N-dimethylaniline based chromophores. *Opt. Mater* **2011,** *33* (3), 336-345.
22. Ashwell, G. J.; Mohib, A., Improved molecular rectification from self-assembled monolayers of a sterically hindered dye. *J. Am. Chem. Soc* **2005,** *127* (46), 16238-16244.

23. Dondoni, A.; Massi, A.; Minghini, E.; Bertolasi, V., Dihydropyridine C-Glycoconjugates by Hantzsch Cyclocondensation. Synthesis of a C (6)-Glycosylated Nifedipine Analogue. *Helv. Chim. Acta* **2002,** *85* (10), 3331-3348.
24. Saunders, J., Top Drugs: Top Synthetic Routes. *Oxford Chemistry Primers* **2002,** *90* (1), ALL-ALL.
25. Taylor Jr, R.; Markley, E.; Ellenbogen, L., The inhibition of monoamine oxidase by styrylquinoliniums. *Biochem. Pharmacol.* **1967,** *16* (1), 79-86.
26. Kumar, R.; Långström, B.; Darreh-Shori, T., Novel ligands of Choline Acetyltransferase designed by in silico molecular docking, hologram QSAR and lead optimization. *Sci Rep* **2016,** *6*, 31247.
27. Fortuna, C. G.; Barresi, V.; Musso, N.; Musumarra, G., Synthesis and applications of new trans 1-indolyl-2-(1-methyl pyridinium and quinolinium-2-yl) ethylenes. *Arkivoc* **2009,** *8*, 222-229.
28. Noor, E. A.; Al-Moubaraki, A. H., Thermodynamic study of metal corrosion and inhibitor adsorption processes in mild steel/1-methyl-4 [4'(-X)-styryl pyridinium iodides/hydrochloric acid systems. *Mater. Chem. Phys.* **2008,** *110* (1), 145-154.
29. McDonagh, C.; Burke, C. S.; MacCraith, B. D., Optical chemical sensors. *Chem. Rev* **2008,** *108* (2), 400-422.
30. Wang, M.; Gao, M.; Miller, K. D.; Sledge, G. W.; Hutchins, G. D.; Zheng, Q.-H., Simple synthesis of carbon-11 labeled styryl dyes as new potential PET RNA-specific, living cell imaging probes. *Eur. J. Med. Chem.* **2009,** *44* (5), 2300-2306.
31. Jones, G., The K noevenagel Condensation. *Org. React.* **2004,** *15*, 204-599.
32. Ieda, N.; Nakagawa, H.; Horinouchi, T.; Peng, T.; Yang, D.; Tsumoto, H.; Suzuki, T.; Fukuhara, K.; Miyata, N., Peroxynitrite generation from a NO-releasing nitrobenzene derivative in response to photoirradiation. *ChemComm* **2011,** *47* (22), 6449-6451.
33. Drygin, D.; Lin, A.; Bliesath, J.; Ho, C. B.; O'Brien, S. E.; Proffitt, C.; Omori, M.; Haddach, M.; Schwaebe, M. K.; Siddiqui-Jain, A., Targeting RNA polymerase I with an oral small molecule CX-5461 inhibits ribosomal RNA synthesis and solid tumor growth. *Cancer Res.* **2011,** *71* (4), 1418-1430.
34. Bywater, M. J.; Poortinga, G.; Sanij, E.; Hein, N.; Peck, A.; Cullinane, C.; Wall, M.; Cluse, L.; Drygin, D.; Anderes, K., Inhibition of RNA polymerase I as a therapeutic strategy to promote cancer-specific activation of p53. *Cancer cell* **2012,** *22* (1), 51-65.
35. Reichardt, C.; Welton, T., *Solvents and solvent effects in organic chemistry*. John Wiley & Sons: 2011.
36. Sheely, M. L., Glycerol viscosity tables. *Ind Eng Chem* **1932,** *24* (9), 1060-1064.
37. Saady, A.; Böttner, V.; Meng, M.; Varon, E.; Shav-Tal, Y.; Ducho, C.; Fischer, B., An oligonucleotide probe incorporating the chromophore of green fluorescent protein is useful for the detection of HER-2 mRNA breast cancer marker. *Eur. J. Med. Chem.* **2019,** *173 (2019): 99-106*.
38. King, M. A., Detection of dead cells and measurement of cell killing by flow cytometry. *J. Immunol. Methods* **2000,** *243* (1-2), 155-166.
39. Peltonen, K.; Colis, L.; Liu, H.; Jäämaa, S.; Moore, H. M.; Enbäck, J.; Laakkonen, P.; Vaahtokari, A.; Jones, R. J.; af Hällström, T. M., Identification of novel p53 pathway activating small-molecule compounds reveals unexpected similarities with known therapeutic agents. *PloS one* **2010,** *5* (9), e12996.
40. Colis, L.; Peltonen, K.; Sirajuddin, P.; Liu, H.; Sanders, S.; Ernst, G.; Barrow, J. C.; Laiho, M., DNA intercalator BMH-21 inhibits RNA polymerase I independent of DNA damage response. *Oncotarget* **2014,** *5* (12), 4361.
41. Sheinberger, J.; Shav-Tal, Y., mRNPs meet stress granules. *FEBS lett* **2017,** *591* (17), 2534-2542.
42. Lu, Y.-J.; Deng, Q.; Hu, D.-P.; Wang, Z.-Y.; Huang, B.-H.; Du, Z.-Y.; Fang, Y.-X.; Wong, W.-L.; Zhang, K.; Chow, C.-F., A molecular fluorescent dye for specific staining and imaging of RNA in live cells: a novel ligand integration from classical thiazole orange and styryl compounds. *ChemComm* **2015,** *51* (83), 15241-15244.
43. Li, Q.; Kim, Y.; Namm, J.; Kulkarni, A.; Rosania, G. R.; Ahn, Y.-H.; Chang, Y.-T., RNA-selective, live cell imaging probes for studying nuclear structure and function. *Chem. Bio* **2006,** *13* (6), 615-623.
44. Bohländer, P. R.; Wagenknecht, H. A., Synthesis of a Photostable Energy-Transfer Pair for "DNA Traffic Lights". *Eur. J. Org. Chem.* **2014,** *2014* (34), 7547-7551.
45. Kamentsky, L.; Jones, T. R.; Fraser, A.; Bray, M.-A.; Logan, D. J.; Madden, K. L.; Ljosa, V.; Rueden, C.; Eliceiri, K. W.; Carpenter, A. E., Improved structure, function and compatibility for CellProfiler: modular high-throughput image analysis software. *Bioinformatics* **2011,** *27* (8), 1179-1180.

GRAPHICAL ABSTRACT

(E)-2-(3,5-Difluoro-4-hydroxystyryl)-1,4-dimethylpyridinium iodide, **12e,** is an attractive staining reagent for visualizing and assessing rRNA in both fixed and living cells.

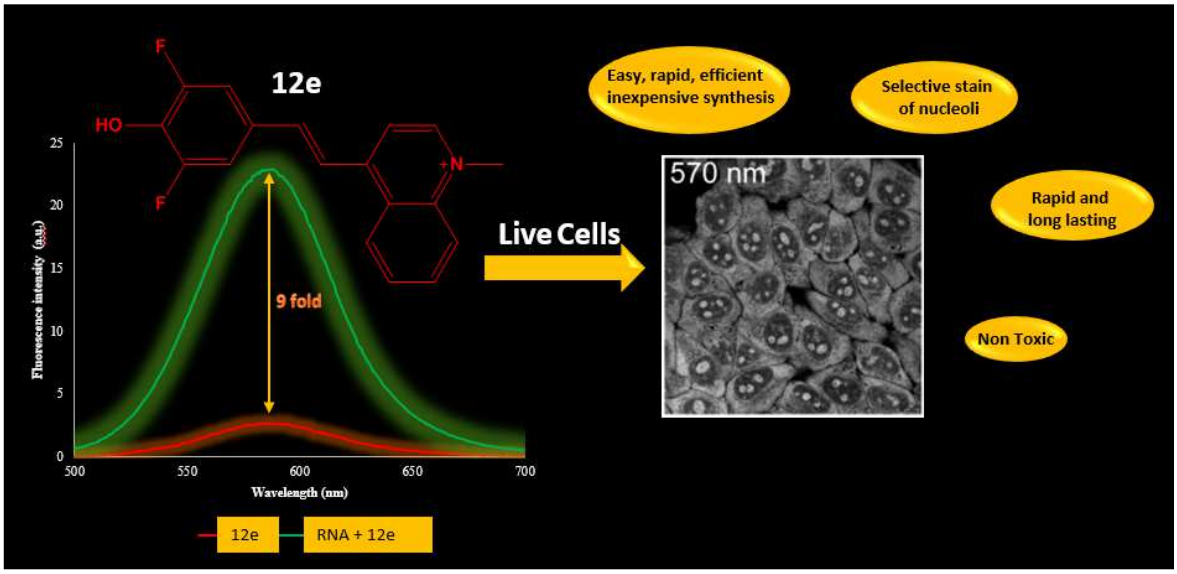

Keywords: fluorescence, flow cytometry, Knoevenagel condensation, live cells, microwave chemistry, microscopy, styryl quinolinium dyes.

Journal Pre-proof

Conflict of interest

The authors declare no conflicts of interest

Applying styryl quinolinium fluorescent probes for imaging of ribosomal RNA in living cells

Abed Saady[a], Eli Varon[b], Avi Jacob[b], Yaron Shav-Tal[b] and Bilha Fischer[a]*

[a] Department of Chemistry, Bar-Ilan University, Ramat-Gan 52900, Israel.

[b] Faculty of Life Sciences & Institute of Nanotechnology, Bar-Ilan University, Ramat-Gan 52900, Israel.

* Corresponding author. Fax: 972-3-6354907. Tel: 972-3-5318303.

Bar-Ilan University, Ramat-Gan 52900, Israel

E-mail: Bilha.fischer@biu.ac.il

Journal Pre-proof